



Published in final edited form as:

*Cardiovasc Eng Technol*. 2010 September ; 1(3): 179–193. doi:10.1007/s13239-010-0020-8.

## Influence of Electromechanical Activity on Cardiac Differentiation of Mouse Embryonic Stem Cells

Worawan Limpitikul<sup>1</sup>, Nicolas Christoforou<sup>2</sup>, Susan A. Thompson<sup>1</sup>, John D. Gearhart<sup>3</sup>, Leslie Tung<sup>1</sup>, and Elizabeth A. Lipke<sup>4</sup>

<sup>1</sup>Department of Biomedical Engineering, Johns Hopkins University School of Medicine, Baltimore, MD 21205, USA

<sup>2</sup>Department of Biomedical Engineering, Duke University, Durham, NC 27708, USA

<sup>3</sup>Institute for Regenerative Medicine, University of Pennsylvania, Philadelphia, PA 19104, USA

<sup>4</sup>Department of Chemical Engineering, Auburn University, Auburn, AL 36849, USA

### Abstract

During differentiation, mouse embryonic stem cell-derived cardiomyocytes (mESC-CMs) receive electromechanical cues from spontaneous beating. Therefore, promoting electromechanical activity via electrical pacing or suppressing it by drug treatment might affect the cellular functional development. Electrical pacing was applied to confluent monolayers of mESC-CMs during late-stage differentiation (days 16–18). Alternatively, spontaneous contraction was suppressed by (a) blocking ion currents with CsCl (HCN channel), trazodone (T-type Ca<sup>2+</sup> channel), or both CsCl and trazodone on days 11–18; or (b) applying blebbistatin (excitation–contraction uncoupler) on days 11–14. Electrophysiological properties and gene expression were examined on day 19 and 18, respectively. Optical mapping revealed no significant difference in conduction velocity (CV) in paced vs. non-paced monolayers, nor were there significant changes in gene expression of connexin-43, Na–Ca exchanger (NCX), or myosin heavy chain (MHC). However, CV variability among differentiation batches and CV heterogeneity within individual monolayers were significantly lower in paced mESC-CMs. Alternatively, while the four drug treatments suppressed contraction with varying degrees (up to complete inhibition), there was no significant difference in CV for any of the treatments compared with controls. Trazodone treatment significantly reduced CV variability as compared to controls, whereas CsCl treatment significantly reduced CV heterogeneity. Distinct changes in gene expression of connexin-43, MHC, HCN1, Cav3.1/3.2 were not observed. Electrical pacing, but not suppression of spontaneous contraction, during late-stage differentiation reduces the intrinsic variability of CV among differentiation batches and across individual monolayers, which can be beneficial in the application of ESCs for myocardial tissue repair.

Address correspondence to Leslie Tung, Department of Biomedical Engineering, Johns Hopkins University School of Medicine, Baltimore, MD 21205, USA. ltung@jhu.edu.

### ELECTRONIC SUPPLEMENTARY MATERIAL

The online version of this article (doi:10.1007/s13239-010-0020-8) contains supplementary material, which is available to authorized users.

## Keywords

Electrical stimulation; Electrophysiology; Cell culture; Optical mapping; Cardiac regeneration

---

## INTRODUCTION

Heart disease is the number one cause of death in the United States, and in 2006, accounted for one in every 3.8 deaths.<sup>14</sup> Recognizing the limited ability of cardiac tissue to regenerate after injury, an alternative approach to conventional treatments such as drugs or cardiac assist devices is cell therapy, in which new cells are engrafted into the area of damaged cardiac tissue. One of the promising cell sources for cardiac regeneration is embryonic stem cells (ESCs), which can be differentiated to become cardiomyocytes. Successful implementation of this approach, however, requires a better understanding of the biochemical and physical cues essential for cardiac differentiation, and importantly, how to better manage the phenotypic variation that cardiomyocytes have both within batches and among different batches when differentiated from ESCs. The research results reported here provide some new insight into these relationships, specifically examining the role of electromechanical signaling on functional development and electrophysiological phenotypic variation of mouse embryonic stem cell-derived cardiomyocytes (mESC-CMs).

For more mature cells grown in culture, electromechanical cues are undoubtedly important. Continuous electrical pacing of newborn rat cardiomyocytes for at least 24 h increased cell elongation, upregulated contractile [ $\alpha$ - and  $\beta$ -myosin heavy chain (MHC)] and electrical (gap junction connexin-43) proteins, and increased functionality (maximum capture rate—the rate at which cells can be stimulated most rapidly without losing 1:1 response).<sup>2,3,16,27</sup> In non-cardiac cells, continuous electrical pacing increased the proliferation of skeletal myoblasts<sup>26</sup> and induced partial differentiation of human and mouse fibroblast cell lines to the cardiac phenotype.<sup>8</sup>

Spontaneous activity in ESCs is associated with cardiomyocyte differentiation, but the role that this beating may play in the differentiation process has not been given much attention.<sup>13</sup> Increases in the number and size of beating foci in mouse embryoid bodies (EBs) have been shown in response to application of a single electric field pulse.<sup>29</sup> Continuous electrical stimulation of mouse embryonic stem cells (mESCs) for 4 days at a 1 Hz pacing rate affected the proportion of cardiomyocytes to ESCs (differentiation yield).<sup>5</sup> Moreover, continuous electrical stimulation of human mesenchymal stem cells for 1–3 weeks at 0.5 Hz pacing rate also induced partial differentiation into cardiomyocytes.<sup>9</sup> However, no studies have yet investigated whether electrical stimulation can also affect the phenotypic variation that occurs even within the cardio-myocyte lineage of cells that are obtained from different differentiation batches of mESCs. Experiments directed at this question will enhance our ability to design biomimetic exogenous pacing protocols to guide cardiac differentiation.

An alternative strategy for determining the importance of electromechanical cues on cardiac differentiation is to suppress the intrinsic spontaneous activity either by suppressing pacemaking transmembrane ion currents or decoupling contraction from excitation. During the intermediate and late stages of mESC differentiation into cardiomyocytes (days 10–19),

automaticity has been previously attributed to the T-type  $\text{Ca}^{2+}$  current,<sup>35</sup> pacemaker current through HCN channels,<sup>20</sup> or both.<sup>34</sup> In separate studies, automaticity has also been attributed to IP<sub>3</sub>-mediated release of  $\text{Ca}^{2+}$  from intracellular stores rather than to functional expression of ion channels.<sup>7,18</sup> While pacemaker currents have been identified in single embryonic stem cell-derived cardiomyocytes (ESC-CMs) by patch clamp studies,<sup>22,34</sup> no studies have been performed that investigated the effects of long-term suppression of pacemaker currents and spontaneous contraction on cardiac differentiation of ESCs.

Thus, this study aims to investigate the effects of electromechanical cues on the electrophysiological characteristics of populations of cardiomyocytes differentiated from mESCs by (1) intensifying the degree of signaling via continuous electrical pacing and (2) suppressing signaling by inhibiting electrical activity via blockers of pacemaking ion channels or by inhibiting contraction by excitation–contraction uncouplers. This study also shows, for the first time, that mESC-CMs can form tissue-scale confluent monolayers whose electrophysiological properties can be studied via optical mapping.

## MATERIALS AND METHODS

### Vector Construction

All cells used in all experiments came from a single clone of mESCs with an  $\alpha$ -MHC promoter driving a neomycin resistance gene. The  $\alpha$ -MHC promoter element has been previously utilized by other groups for the purpose of deriving a pure population of cardiomyocytes from differentiating ESCs. Klug et al.<sup>19</sup> first described the construction and utilization of a similar DNA plasmid ( $\alpha$ -MHC<sub>promoter</sub>-NeoR/PGK<sub>promoter</sub>-HygroR) for the purpose of selecting cardiomyocytes. Following selection with neomycin for 8 days they were able to derive cardiomyocytes with a purity of 99.6%. Kolossov et al.<sup>21</sup> also utilized this promoter to select cardiomyocytes using puromycin selection. They reported cardiomyocyte purity of >99% following addition of puromycin in their cultures of differentiating ESCs.

The mouse promoter (kind gift of Drs. J. Gullick and J. Robbins) of the  $\alpha$ -MHC gene (5453 bp, U71441) was cloned in the 5' end of the neomycin phospho-transferase gene. For the purpose of this experiment, two plasmids were utilized: Polymerase II<sub>promoter</sub>-Hygromycin Phosphotransferase, the plasmid which allowed us to select for ESC clones which were stably transfected, and  $\alpha$ -MHC<sub>promoter</sub>-neomycin phospho-transferase, the plasmid which allowed us to select for Myh6<sup>+</sup> cells. Prior to transfection both plasmids were linearized using XmnI and combined with a ratio of 10:1 ( $\alpha$ -MHC-NeoR: PolII-HygroR).

### Cell Transfection and Clone Selection

mESCs (D3 line) were cultured on gelatin in the presence of leukemia inhibitory factor (LIF;  $10^3$  U/mL). For the purpose of transfection, the cells were trypsinized and resuspended in 800  $\mu\text{L}$  of  $\text{Ca}^{2+}/\text{Mg}^{2+}$  solution. Then, 10  $\mu\text{g}$  of the DNA mix was added to the cells, and the combined solution was placed into a 4-mm electroporation cuvette. The cells were electroporated in a Biorad Gene Pulser Xcell (240 V/500  $\mu\text{F}$ ) and re-plated onto  $\gamma$ -irradiated hygro-resistant primary mouse embryonic fibroblasts (PMEFs) in a 10-cm diameter tissue culture

plate. The next day hygromycin (200 µg/mL) was added to the ESC medium, and the antibiotic selection lasted for 7 days. In order to ensure that a derived clone could provide selection of pure cardiomyocytes, at least 50 clones or colonies were picked 7–10 days following electroporation, and specificity of the promoter element was tested.

After expansion, 90% of the cells from each colony were cryopreserved in their undifferentiated state and 10% of the cells were differentiated using the hanging droplet technique. Neomycin was added when spontaneously contracting cells were observed. One of several clones in which only spontaneously contracting cells survived following neomycin selection was used for all subsequent experiments. For the selected clone: (1) following prolonged culture post-selection with neomycin, no colonies resembling undifferentiated ESCs were detected; (2) when staining the cells with antibodies specific for cardiomyocytes, every cell stained positive (see “Results” section); and (3) following RT-PCR analysis for cells of other lineages (endoderm, ectoderm), expression of such markers was not detected. Moreover, RT-PCR analysis for Oct4, Sox2, and Nanog (proteins expressed by undifferentiated ESCs) was negative (data not shown).

### Cell Differentiation

The genetically modified mESCs were expanded on a feeder layer of PMEFs in the presence of 1 µL/mL LIF (Chemicon, Millipore, Billerica, MA). Feeder layer subtraction was performed, and the mESCs were expanded for an additional 24–48 h on gelatin-coated plates. To initiate differentiation of the mESCs into cardiomyocytes (mESC-CMs), LIF was removed and EBs of mESCs were formed by the hanging droplet method<sup>32</sup> (day 0). The concentration of cell suspension used in this experiment was  $5 \times 10^4$  cells/mL (1000 cells per 20-µL droplet). On day 3, EBs were transferred from the hanging droplets and suspended in culture medium including 100 µg/mL ascorbic acid. On day 5, EBs were transferred to gelatin-coated plates. From day 6 to day 9, neomycin was added to the culture medium to select for mESC-CMs. On day 9, EBs were dissociated into single cells and seeded on 21-mm diameter fibronectin-coated polyvinyl chloride coverslips. Neomycin selection was restarted on day 11 and completed on day 14 (Fig. 1). Monolayers that were confluent on day 18 were included in subsequent analyses. Standard culture medium consisted of pre-screened 10% FBS (Atlanta Biologicals Inc, Lawrenceville, GA), 85% DMEM (Gibco, Invitrogen, Carlsbad, CA), supplemented with 1% (v/v) Gluta-Max-1 (Gibco), 1% (v/v) MEM non-essential amino acids (Gibco), 1% (v/v) sodium pyruvate (Gibco), 1 µL/mL 2-mercaptoethanol (Gibco), 50 µL/100 mL gentamicin sulfate (Lonza Biowhittaker, Basel, Switzerland). All studies were done using the same lot of FBS.

### Promotion of Electromechanical Activity by Electrical Pacing

Threshold for electrical pacing was determined by the minimum voltage rendering one-to-one capturing of mESC-CMs by 40-ms duration pulses at 3 Hz and ranged from 1.67 to 3.0 V/cm. Monolayers with spontaneous beating rate over 3 Hz were excluded from the experiment. Monolayers of mESC-CMs were paced at 0.17 V/cm above threshold at 3 Hz for 7 h/day on days 16–18 (the earliest time at which cells could be consistently paced) prior to the day of mapping. Maintenance of pacing capture was verified daily by visual inspection. A stimulation circuit was constructed, based on Sathaye’s design.<sup>28</sup> Bidirectional

rectangular impulses were used to prevent the accumulation of free radicals and ions caused by the electrical impulses. The pacing chamber contained electrodes made of 0.02 in. diameter graphite rods. Sixteen electrodes were connected in series and held down to the bottoms of the wells by 52-gauge Teflon-coated platinum wire. Prior to cell stimulation, the electrodes were sterilized by sonicating in 70% ethanol and autoclaving.

### Suppression of Electromechanical Activity by Drug Treatment

mESC-CMs were treated with either 10  $\mu$ M blebbistatin (an excitation-contraction uncoupler) on days 11–14,<sup>6</sup> 1 mM CsCl (HCN channel blocker) on days 11–18,<sup>34</sup> 50  $\mu$ M trazodone (T-type Ca<sup>2+</sup> channel blocker) on days 11–18,<sup>22</sup> or the combination of 1 mM CsCl and 50  $\mu$ M trazodone on days 11–18 (Fig. 1). Sustained exposure to blebbistatin caused the mESC-CMs to retract from each other, so blebbistatin was removed on day 15, after which the mESC-CMs expanded back and recoupled to become confluent by the day of mapping. The rate of spontaneous contraction was observed visually. The number of beats was counted during a 20-s interval.

### Optical Mapping

Monolayers of mESC-CMs were optically mapped on day 19 for the electrical pacing experiments and on day 18 for the suppression of spontaneous contraction experiments. Each monolayer was stained with voltage-sensitive dye (10  $\mu$ M di-4-ANEPPS) and stimulated with a point electrode. Optical signals were captured by an array of 253 photodiodes with 1 mm spatial resolution.<sup>30</sup> Tyrode's solution for the mapping experiments contained (in mM): NaCl 135, KCl 5.4, MgCl<sub>2</sub> 2, CaCl<sub>2</sub> 1.8, glucose 10, HEPES 10 at pH 7.4 (NaOH) and 37 °C. LabVIEW (National Instruments, Austin, TX) was used to collect data, and custom MATLAB (The Mathworks, Natick, MA) scripts were used to calculate conduction velocity (CV) and the heterogeneity index (HI) of the propagating wave. To calculate HI, the difference in activation times between a specific recording site and its six surrounding sites is determined, and the maximum number is chosen to represent the phase delay for that channel. A histogram of phase delays from all 253 sites is plotted, and HI is calculated by dividing  $P_{95}-P_5$  by  $P_{50}$ , where  $P_x$  represents the value at the xth percentile.<sup>23</sup>

### Immunohistochemistry

Immunohistochemistry was performed on mESC-CMs after they were optically mapped. Monolayers were fixed either with 50:50 acetone/ethanol or 5% paraformaldehyde. Cells were permeabilized with 0.2% v/v Triton X in PBS containing 1% w/v bovine serum albumin. Monolayers were blocked with 3% FBS in PBS. Primary antibodies used were monoclonal mouse IgG1 anti-connexin-43 (1:200) (Chemicon), monoclonal mouse IgG1 anti- $\alpha$ -sarcomeric actinin (1:400) (Sigma-Aldrich), monoclonal mouse IgM anti-MHC (1:500) (Abcam, Cambridge, MA), monoclonal mouse IgG2b anti cardiac troponin I (1:500) (US Biological, Swampscott, MA). Secondary antibodies were Alexa Fluor 568 goat anti-mouse IgG1 (1:200) and Alexa Fluor 488 goat anti-mouse IgM (1:200) (all from Invitrogen, Carlsbad, CA). Then, monolayers were counterstained for nuclei with 4,6'-diamidino-2-phenylindole (DAPI, Invitrogen). Samples were mounted with Prolong Gold Antifade mounting media (Invitrogen). Mounted samples were imaged with a Zeiss 510 META confocal microscope together with an inverted fluorescence microscope (Nikon Eclipse

TE2000-U) with appropriate filter cubes (Chroma Technology Corporation) and with phase contrast. Image analysis, including image overlay, nucleus and cell counting, was performed using ImageJ software (NIH).

### Gene Expression

Samples of total RNA were collected on day 18 for the electrical pacing experiments and on day 17 for the suppression of spontaneous contraction experiments, using RNeasy kit (Qiagen, Hilden, Germany). First-strand cDNA was made using SuperScript III First-Strand Synthesis System for RT-PCR (Invitrogen). The primers used are given in Table 1. The cycle used for RT-PCR was as follows: initial denaturation at 94 °C (5 min), 35 cycles of denaturation at 94 °C (1 min), primer annealing at 55 °C (40 s), primer extension at 72 °C (1 min), and substance clearance at 72 °C (10 min). Products were removed and visualized by gel electrophoresis. Real-time RT-PCR was done with a Bio-Rad iCycler iQ Real-Time PCR Detection System with iCycler v.3.1 software (Bio-Rad Laboratories, Hercules, CA), using Power SYBR Green Master Mix (Invitrogen), and following manufacturer instructions. Levels of expression were calculated by fitting unknown samples to a standard curve.

### Statistical Analysis

CV and HI of control and treatment groups were compared using a linear mixed-effect model. Variability of CVs for control monolayers among the differentiation batches of mESC-CMs and variability of CVs for treated monolayers among the differentiation batches of mESC-CMs were analyzed using a one-way ANOVA. Statistical differences in CV variance between the control monolayers and the treatment monolayers were determined using Levene's test, which has the null hypothesis that the population variances are equal. To compare variance between the paced and control monolayers, three CV measurements per monolayer, taken minimally 60° apart (for circular wave propagation), were taken to be independent for purposes of this analysis. Number of cells, area of cells, and number of nuclei were compared using two-way Student's *t* test. Values of  $p < 0.05$  were considered to be significant. Error bars represent standard deviations.

## RESULTS

### Monolayers of mESC-CMs

To form mESC-CM monolayers, EBs were dissociated into single cell suspension of mESC-CMs on day 9 and seeded on fibronectin-coated polyvinyl chloride coverslips. Neomycin selection was continued for additional 4 days (Fig. 1). Before day 18, these tissue-scale (3.8 cm<sup>2</sup>) monolayers of mESC-CMs achieved confluency (Fig. 2a). That is, instead of having multiple beating foci, confluent monolayers of mESC-CMs contracted synchronously, demonstrating good electrical coupling between adjacent cells (Online Resource 1). These monolayers could be optically mapped (Fig. 2b) for measurements of CV (Online Resources 2 and 3).

### Electrical Pacing

**Electrical Properties of Paced mESC-CM Monolayers**—On day 19, CVs of electrical wave fronts propagating across mESC-CM monolayers were measured by



analyzing the isochrone maps (Fig. 2c). CVs ranged from 2.0 to 7.5 cm/s at a 4-Hz stimulation rate for control (non-paced conditions) and 3.0 to 7.0 cm/s for paced mESC-CMs. Statistical analysis indicated no significant difference in CVs for paced vs. control conditions (linear mixed-effect model).

Electrical pacing, however, substantially reduced the intrinsic variability of CVs among differentiation batches. Although the mean CVs of control mono-layers were significantly different among batches, the mean CVs for paced monolayers were not (one-way ANOVA)—i.e., with electrical pacing, CVs were less dispersed (Fig. 3a). Thus, electrical pacing resulted in less batch-to-batch (i.e., differentiation-to-differentiation) variation in the mESC-CM monolayers. In addition, variance of CV for paced monolayers was statistically less than variance of CV for control monolayers (Levene's test,  $p < 0.05$ ). Furthermore, electrically paced mESC-CM monolayers showed more homogeneous propagation across the individual monolayer than did control monolayers (Fig. 2c, Online Resources 2 and 3). The HI, which measures variability of CVs within individual monolayers, was significantly lower in paced mESC-CMs than that for controls ( $1.37 \pm 0.45$  vs.  $1.78 \pm 0.87$ , respectively) (Fig. 3b).

Since cell density could affect CV, cell density in each group was quantified. No significant difference was observed in the number of cells per area between the treatment and the control groups:  $163.1 \pm 30.9$  cells per visual field ( $9461 \mu\text{m}^2$ ) for the control and  $150.7 \pm 25.3$  cells per visual field for the paced group.

**Gene Expression of Paced mESC-CMs**—Connexin-43 and the Na–Ca exchanger (NCX) are important cardiac function genes, whereas  $\alpha$ - and  $\beta$ -myosin are important cardiomyocyte markers. Both paced and control mESC-CM monolayers expressed connexin-43, NCX, and  $\alpha$ - and  $\beta$ -MHC as shown by measuring the levels of mRNA for these respective genes. Based on reverse transcription PCR (RT-PCR), there was no apparent change in gene expression for NCX,  $\alpha$ - and  $\beta$ -myosin in paced mESC-CM mono-layers, compared with the control ( $n = 3$  differentiations) (Online Resource 4). However, real-time (quantitative) RT-PCR of connexin-43 showed mixed results ( $n = 3$  differentiations). There was a 2- and 2.5-fold increase in expression of connexin-43 for paced over control monolayers in two differentiation batches and no change in expression of connexin-43 in one differentiation batch. (Online Resource 5). Immunohistochemistry was performed to confirm the presence and localization of the products of connexin-43 (Fig. 4 and Online Resource 6) and MHC genes (data not shown).

**Immunohistochemistry**—Expression of the gap junction protein, connexin-43, at the cell border is often used as a measure of the extent of electrical coupling between adjoining cardiomyocytes, while the staining of  $\alpha$ -sarcomeric actinin and cardiac troponin I, cardiomyocyte structural protein, represents the morphology of cardiomyocytes. Figure 4 shows immunostaining of mESC-CMs for connexin-43 (left column) and  $\alpha$ -sarcomeric actinin (right column). The distribution of both proteins was similar for control and paced mESC-CMs. The morphology of the mESC-CMs was also similar for control and paced mESC-CMs. Also notice the presence of cells with two nuclei in the monolayers (examples of such cells are indicated with yellow arrows in Fig. 4 right column). There were  $13.4 \pm 2.2\%$  and  $13.7 \pm 2.3\%$  of such cells in control and paced groups, respectively. The number

of binucleated cells was not significantly different between groups (five samples per differentiation, two differentiations per treatment/control group). Expression of cardiac troponin I is shown in Online Resource 6.

### Suppression of mESC-CM Contraction

**Sources of Spontaneous Contraction in Differentiating mESC-CMs—**To suppress spontaneous contraction of mESC-CMs by blocking pacemaker currents, mESC-CMs were treated on days 11–18 with either 1 mM CsCl (HCN channel blocker), 50 IM trazodone (T-type  $\text{Ca}^{2+}$  channel blocker), or a combination of CsCl and trazodone (Fig. 5). Even during the initial treatment days, i.e., intermediate-stage differentiation (days 11–13), spontaneous contraction was only partially suppressed by CsCl. In contrast, trazodone completely suppressed spontaneous contraction during intermediate-stage differentiation. However, during days 14–18, i.e., late-stage differentiation, neither CsCl alone nor trazodone alone was able to completely suppress spontaneous contraction. However, a combination of CsCl and trazodone completely suppressed contraction during the entire time course (days 13–18). These results suggest that T-type  $\text{Ca}^{2+}$  current is a major source of spontaneous activity during the intermediate stage of differentiation. In late-stage differentiation, however, the role of HCN current becomes more prominent and together with T-type  $\text{Ca}^{2+}$  current, contributes to the spontaneous activity.

To examine the relative importance of electrical signaling as compared to mechanical contraction in guiding mESC-CM differentiation, an excitation–contraction uncoupler, blebbistatin, was employed. Contraction could also be completely suppressed by blebbistatin when applied on days 11–14 (Fig. 5). After washout of blebbistatin on day 15, spontaneous contraction of mESC-CMs returned and increased with time, but the rate of spontaneous contraction was still slower than in untreated controls. Therefore, uncoupling excitation–contraction had a significant effect on the spontaneous beating activity of the cells.

**Electrical Properties of mESC-CM Monolayers with Suppressed Spontaneous Contraction—**At a 5-Hz stimulation rate, CVs of control mESC-CM monolayers ranged from 2.0 to 5.5 cm/s while CVs of blebbistatin-treated mESC-CMs ranged from 2.5 to 5.0 cm/s (Fig. 6a). CVs of CsCl-treated and trazodone-treated mESC-CMs were similar, ranging from 2.0 to 5.5 cm/s and 2.5 to 3.5 cm/s, respectively. At a 6-Hz stimulation rate, CVs of control mESC-CMs ranged from 1.5 to 5.0 cm/s while CVs of CsCl and trazodone-treated mESC-CMs ranged from 2.0 to 5.0 cm/s. No significant difference in CVs was found in any of the four treatments compared with control (linear mixed-effect model). In terms of variation among differentiation batches, neither mean CVs of controls nor mean CVs of drug-treated mESC-CMs were significantly different among batches (one-way ANOVA) so reduction of variance in treatment groups was inconclusive based on this statistical test. However, when comparing control CV variance and drug treatment CV variance, there was a significant difference between trazodone-treated monolayers and control monolayers (Levene's test,  $p < 0.0001$ ). Therefore, whether suppression of spontaneous activity affected batch-to-batch variation was inconclusive, with only trazodone treatment showing a significant reduction in CV variability as compared to control.



The variability of CVs within each monolayer of mESC-CMs was also determined at a 6-Hz stimulation rate for CsCl and trazodone-treated mESC-CMs and at a 5-Hz stimulation rate for the other three treatment groups (Fig. 6b). Heterogeneity of CVs across control and drug-treated mESC-CM monolayers from the same differentiation batch were compared. HI's of drug-treated vs. control were: blebbistatin:  $1.26 \pm 0.43$  vs.  $1.56 \pm 0.67$ ; CsCl:  $1.39 \pm 0.32$  vs.  $1.53 \pm 0.63$ ; trazodone:  $1.21 \pm 0.20$  vs.  $1.23 \pm 0.31$ ; CsCl and trazodone:  $1.32 \pm 0.18$  vs.  $1.30 \pm 0.30$ . Only the HI of CsCl-treated mESC-CMs was significantly lower than that of control.

Since cell density could potentially affect CVs, cell density was quantified in all groups. No significant differences were observed in the number of cells per area between any of the treatment groups and the control groups:  $69.4 \pm 12.8$  cells per visual field ( $9461 \mu\text{m}^2$ ) for blebbistatin-treated group,  $82.7 \pm 19.7$  cells per visual field for CsCl-treated group vs.  $71.3 \pm 12.3$  cells per visual field for control group; and  $117.4 \pm 27.2$  cells per visual field for trazodone-treated group vs.  $101.4 \pm 24.6$  cells per visual field for control group (five samples per differentiation, two differentiations per treatment/control group).

#### **Gene Expression of mESC-CMs with Suppressed Spontaneous Contraction—**

Gene expression level of ion channels was measured to determine whether suppression of a specific current could affect the expression level of other types of ion channels and of itself. RT-PCR on connexin-43,  $\alpha$ - and  $\beta$ -MHC, HCN1, and the predominant subtypes of T-type  $\text{Ca}^{2+}$  channels (Cav3.1 and Cav3.2) was performed on mRNA samples from three differentiations. Each differentiation contained control, CsCl-, trazodone-, and blebbistatin-treated mESC-CMs. There was no distinct trend in the change of the expression level of these genes (Online Resource 7). Immunohistochemistry was performed that confirmed the presence and localization of the products of connexin-43 (Fig. 7) and MHC genes (data not shown).

#### **Morphological Changes in Blebbistatin-Treated but not in CsCl- or Trazodone-Treated mESC-CMs—**

Morphological changes were observed in blebbistatin-treated but not CsCl- or trazodone-treated mESC-CMs. With blebbistatin treatment, mESC-CMs retracted from each other, exhibiting a smaller cell footprint ( $478.5 \pm 76 \mu\text{m}^2$  on day 14,  $n = 8$ ) than in control ( $902.9 \pm 93 \mu\text{m}^2$ ,  $n = 6$ ) (Online Resource 8). However, throughout the drug treatment, the morphology of mESC-CMs in the presence of CsCl or trazodone did not change (Fig. 7, last two rows) and was similar to that of control (Fig. 7, first row). Upon removal of blebbistatin, mESC-CMs expanded back with a rod-shaped morphology, (Fig. 7, second row) which was different from morphology of control and other treatments (Fig. 7, first, third, and fourth row).

Moreover, blebbistatin-treated mESC-CMs also showed apparent local alignment of cells that are confined to small groups of cells (Fig. 7, second row) while the control and other treatment groups (Fig. 7, first, third, and fourth rows) did not. However, the alignment of blebbistatin-treated mESC-CMs did not extend on a global scale (i.e., millimeter or larger) (Online Resource 9). Therefore, the wave propagation remains isotropic at this spatial scale.

Note the presence of mESC-CMs that possessed two nuclei in the monolayers (example of such cells are indicated with yellow arrows in Fig. 7 right column). There were  $13.4 \pm 3.8\%$ ,

14.2 ± 3.6%, 13.3 ± 4.5%, and 14.2 ± 3.9% of such cells in control, blebbistatin-treated, CsCl-treated, and trazodone-treated groups, respectively. The number of binucleated cells was not significantly different between any of the four groups (five samples per differentiation, two differentiations per treatment/control group).

## DISCUSSION

The goal of this study was to determine the importance of electromechanical cues on differentiation and phenotypic electrophysiological variation among different batches of mESC-CMs. mESC were differentiated to become cardiomyocytes and plated to form monolayers. This study demonstrated, for the first time, that mESC-CMs could form tissue-scale (3.8 cm<sup>2</sup>) confluent monolayers which can serve as an experimental model to study the electrophysiological function of mESC-CMs at a tissue level. In this study, electromechanical cues were varied by either introducing electrical pacing or suppressing spontaneous contraction to determine the effect on propagated electrical activity.

Our main finding is that electrical pacing at 3 Hz for 3 days (7 h/day) significantly decreases the variability of CV among different differentiation batches compared with that for control and increases the homogeneity of CVs within individual monolayers of mESC-CMs. There were no apparent changes in the level of expression of NCX, and  $\alpha$ - and  $\beta$ -MHC in paced vs. control mESC-CMs (Online Resource 4). However, real-time RT-PCR showed mixed results in level of expression of connexin-43 (Online Resource 5). On the other hand, we found that in general the suppression of spontaneous contraction by blockers of pacemaker currents or by an excitation-contraction uncoupler did not significantly change the variability among differentiation batches, with the exception of the T-type Ca<sup>2+</sup> channel blocker trazodone, or the heterogeneity of CV within monolayers, with the exception of the HCN channel blocker, CsCl. There was no apparent change in the level of gene expression for  $\alpha$ - and  $\beta$ -MHC, HCN1, or the predominant subtypes of T-type Ca<sup>2+</sup> channels (Cav3.1 and Cav3.2) in drug-treated vs. control mESC-CMs. However, there were mixed results in level of expression of connexin-43 in CsCl-treated mESC-CMs, compared to the control (Online Resource 7). Our spontaneous beating results (Fig. 5) also suggest that on days 11–14 of mESC differentiation, the major source of pacemaker current is the T-type Ca<sup>2+</sup> channel, which transitions to a combination of T-type Ca<sup>2+</sup> and HCN channels on days 14–17.

### Electrical Pacing has Little Effect on Conduction Velocity but Reduces its Variability

Any tissue heterogeneity in electrophysiological properties of the cardiac cells is an important arrhythmic risk factor that can cause conduction block, fragmented wavefronts and fibrillation.<sup>31</sup> In this study, tissue-scale monolayers of mESC-CMs were cultured, and their functional electrical properties were mapped for the first time. CV of both control and paced mESC-CMs varied over a wide range (Fig. 3a), a result that is not surprising given that individual mESC-CM monolayers exhibit a broad range of cardiac subpopulations, including sinus node-like, atrial-like and ventricular-like cells.<sup>15</sup> Another contributing factor is the phenotypic variation among differentiation batches, which might arise either from different proportions of the various cardiac subpopulations or from different levels of gene expression of ion channels and electrogenic ion pumps and exchangers. This large variability

may explain why no statistical difference was found between the CVs of the control and paced groups and why separate differentiation batches of mESC-CMs showed mixed results in terms of increased or decreased CV with pacing when compared to paired unpaced controls.

Despite the lack of statistical change in CV when results from multiple differentiation batches were pooled, electrical pacing reduced the variability of CV among batches of mESC-CMs (Fig. 3a) and the heterogeneity of CV within a given monolayer (Fig. 3b). Improvements in the uniformity of CV may prove to be essential in cardiac tissue engineering, where the goal is to produce a cardiac tissue patch or implant that can be used as a replacement tissue without introducing new risks for arrhythmia that are associated with non-uniform conduction. Furthermore, reduction of variability of CVs of monolayers made from different differentiation batches can lead to better quality control for future, larger-scale production of replacement tissue.

Apart from the issue of heterogeneity of conduction is the magnitude of CV itself. In the embryonic mouse heart, CVs have been measured to be an average of 53 cm/s in the left atrial appendage and 63 cm/s in the right atrial appendage at a 10 Hz stimulus rate (100 ms basic cycle length). However, the CVs in our monolayers of mESC-CMs are an order of magnitude smaller. This may be attributed in part to the late appearance of the fast sodium current ( $I_{Na}$ ) and the inwardly rectifying potassium current ( $I_{K1}$ ) during development,<sup>15</sup> both of which work synergistically to increase the excitatory current needed for fast conduction—the former by increasing the maximum available excitatory current and the latter by hyperpolarizing the resting potential and increasing the availability of  $I_{Na}$ . The lower CV may also be a consequence of the non-physiological culture conditions under which the mESC-CMs are grown. Previous studies have shown the benefits of alignment and incorporation of non-myocyte cell types in engineered cardiac tissues.<sup>4,25,36</sup> The lack of cell alignment and the absence of non-myocyte cardiac cells, due to the  $\alpha$ -MHC selection method, may be contributing factors to the observed slower CVs. Implantation of cardiac tissue patches with such a large discrepancy in CV compared with the host myocardium will result in a region of slowed conduction that can be arrhythmogenic.

One possible mechanism that could explain reduced variability of CV within individual monolayers and among differentiation batches involves NFAT3/calcineurin signaling pathway. Electrical pacing at 2–3 Hz was shown to activate NFAT3/calcineurin pathway<sup>33</sup> of which one downstream effect is increased expression of SERCA2,<sup>1</sup> the most dominant protein for  $Ca^{2+}$  removal in differentiating mESC-CMs.<sup>12</sup> For developing mESC-CMs,  $Ca^{2+}$  in sarcoplasmic reticulum plays two critical roles of contraction and spontaneous excitability.<sup>17</sup> With better  $Ca^{2+}$  handling, paced mESC-CMs could demonstrate more uniform contraction, excitation, and wave propagation.

### **Suppression of Spontaneous Contraction has Little Effect on Conduction Velocity or its Variability**

To determine whether the elimination of spontaneous contraction affects cardiac differentiation, mESC-CMs were cultured in the presence of CsCl (HCN blocker) and/or trazodone (T-type  $Ca^{2+}$  channel blocker) to prevent electrical activity that could initiate

contraction, or with blebbistatin to prevent excitation-contraction coupling. The degree to which contraction was suppressed varied with the intervention that was used (being complete for blebbistatin and the combination of CsCl and trazodone, less so for trazodone alone, and even less for CsCl alone), suggesting that initially (days 11–13) the major source of spontaneous activity is the T-type  $\text{Ca}^{2+}$  channel, and later (days 14–17) it is a combination of T-type  $\text{Ca}^{2+}$  and HCN channels. However, in all cases, CVs were not significantly altered (Fig. 6a). There was also no significant change in the HI of CVs within individual monolayers except with CsCl treatment alone (Fig. 6b). Interestingly, this is the condition that was least effective in suppressing contraction, suggesting that the maintenance of spontaneous contraction, even at a slowed rate (Fig. 5), may serve to reduce CV heterogeneity within a given monolayer.

During blebbistatin treatment, mESC-CMs retracted from each other, demonstrating smaller cell footprints compared to the control. The same effect was previously observed in NRK fibroblast cells.<sup>24</sup> This happened because blebbistatin is a specific inhibitor for myosin II which acts as a crosslinker for actin filaments. Blebbistatin helps relieve the stress imposed by actomyosin cytoskeleton and thus, reducing the adhesive tension, allowing cytoskeleton to reorganize which gave the cells more distinct striation.<sup>10</sup>

## LIMITATIONS

One of the limitations of our experiments is that we applied electrical stimulation only during late-stage differentiation, when the cells could be electrically captured by the stimulation. We do not know if the outcome would be different had stimulation been applied during earlier or even later stages of differentiation. Also, in the electrical stimulation experiments we applied only one suprathreshold strength of electrical field, whereas it has been reported that the strength of electrical field may affect the degree of differentiation.<sup>5</sup> Another potential limitation is that all experiments were performed using one genetically modified clone from one mESC line; it was not feasible within the scope of this study to investigate the potential variability that could occur with use of multiple clones or stem cell lines. Additionally, aside from connexin-43 which was quantified by real-time RT-PCR, reverse transcriptase PCR was used to assess changes in gene expression. Although there were no apparent changes in the expression levels of  $\alpha$ - and  $\beta$ -MHC, HCN1, and the T-type  $\text{Ca}^{2+}$  channels (Cav3.1 and Cav3.2), no major conclusions were drawn from these results due to concerns about assay sensitivity. Further study will be needed to elucidate how changes in gene expression could be contributing to the observed reduction in variability and heterogeneity with electrical pacing. Finally, the suppression of spontaneous contraction was achieved by suppressing ionic pacemaking currents or by using an excitation-contraction inhibitor. However, IP3-mediated release of intracellular  $\text{Ca}^{2+}$  stores are also known to contribute to automaticity of mESC-CMs on days 10–17.<sup>7,18</sup> Whether suppression of intracellular  $\text{Ca}^{2+}$  transients might alter the functional electrophysiological development of the cells is presently unknown.

Therapeutic use of stem cell-derived cardiomyocytes requires that multiple hurdles be overcome. Obtaining cardiomyocytes with homogenous electrophysiological properties is a necessary step in this process to avoid complications of arrhythmias once the cells are

implanted into host myocardium. Even when genetic selection was performed in this study for cells in the cardiac lineage, which should vastly reduce phenotypic variability, significant batch-to-batch variability was still observed in the control monolayers, albeit lessened with electrical pacing. Whether the degree of residual variability is sufficient to avoid arrhythmias remains to be seen. For clinical applications, it will be necessary to avoid the use of foreign genetic material, fibroblast feeder layers, and other animal-derived products in deriving stem cell-derived cardiomyocytes, while at the same time constraining their electrophysiological variability. In addition, such systems will need to be scalable and ideally make use of autologous cells.

## CONCLUSIONS

Increasing the contraction rate of mESC-CMs via electrical pacing has more distinct effects on the differentiation of mESC-CMs than does suppression of spontaneous contraction. Electrical stimulation decreases the variability of CVs across mESC-CM monolayers among different differentiation batches and reduces the heterogeneity of conduction within a given cell monolayer, enabling smoother wave propagation in sheets of cells. This knowledge could possibly be applied to achieve uniform conduction in a future cardiac patch and better quality control for larger-scale production of stem cell-derived cardiomyocytes. Both of these effects would be beneficial in the creation of tissue patches for use in cardiac replacement therapy.

## Acknowledgments

The authors would like to thank Dr. Peter He for providing statistical advice. This work was supported by a Johns Hopkins Provost's Undergraduate Research Award (W.L.), NIH training grant T32-HL07581 (E.A.L.; A. Shoukas, principal investigator), funds from the Johns Hopkins Institute for Cell Engineering (J.G.), NIH R01 HL066239 (L.T.), and grant 0855330E from the Mid-Atlantic Affiliate of the American Heart Association (L.T.).

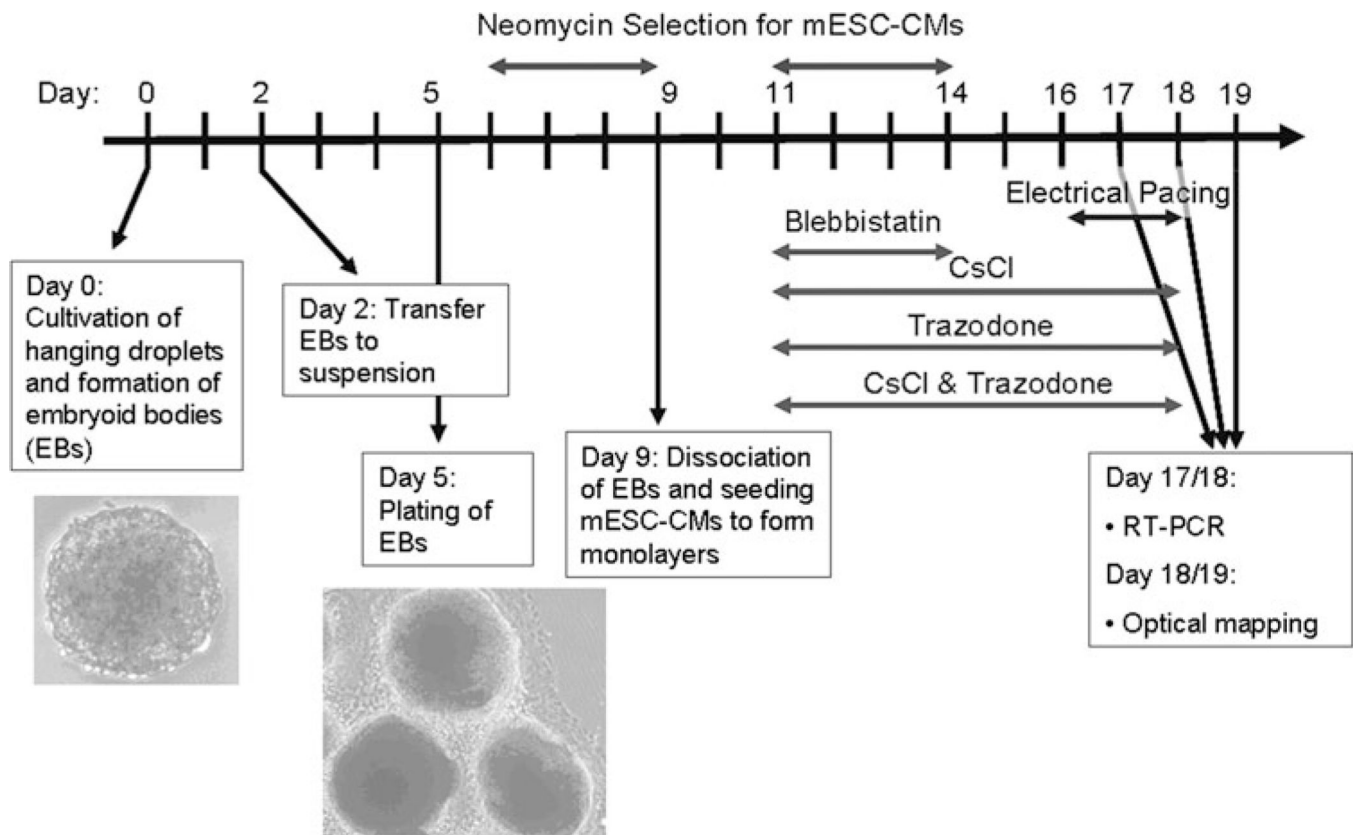
## References

1. Anwar A, Taimor G, Korkusuz H, Schreckenber R, Berndt T, Abdallah Y, Piper HM, Schlüter KD. PKC-independent signal transduction pathways increase SERCA2 expression in adult rat cardiomyocytes. *J. Mol. Cell Cardiol.* 2005; 39:911–919. [PubMed: 16236312]
2. Au HT, Cheng I, Chowdhury MF, Radisic M. Interactive effects of surface topography and pulsatile electrical field stimulation on orientation and elongation of fibroblasts and cardiomyocytes. *Biomaterials.* 2007; 28:4277–4293. [PubMed: 17604100]
3. Berger HJ, Prasad SK, Davidoff AJ, Pimental D, Ellingsen O, Marsh JD, Smith TW, Kelly RA. Continual electric field stimulation preserves contractile function of adult ventricular myocytes in primary culture. *Am. J. Physiol.* 1994; 266:H341–H349. [PubMed: 8304516]
4. Caspi O, Lesman A, Basevitch Y, Gepstein A, Arbel G, Habib IH, Gepstein L, Levenberg S. Tissue engineering of vascularized cardiac muscle from human embryonic stem cells. *Circ. Res.* 2007; 100:263–272. [PubMed: 17218605]
5. Chen MQ, Xie X, Hollis Whittington R, Kovacs GT, Wu JC, Giovangrandi L. Cardiac differentiation of embryonic stem cells with point-source electrical stimulation. *Conf. Proc. IEEE Eng. Med. Biol. Soc.* 2008; 2008:1729–1732. [PubMed: 19163013]
6. Fedorov VV, Lozinsky IT, Sosunov EA, Anyukhovskiy EP, Rosen MR, Balke CW, Efimov IR. Application of blebbistatin as an excitation-contraction uncoupler for electrophysiologic study of rat and rabbit hearts. *Heart Rhythm.* 2007; 4:619–626. [PubMed: 17467631]

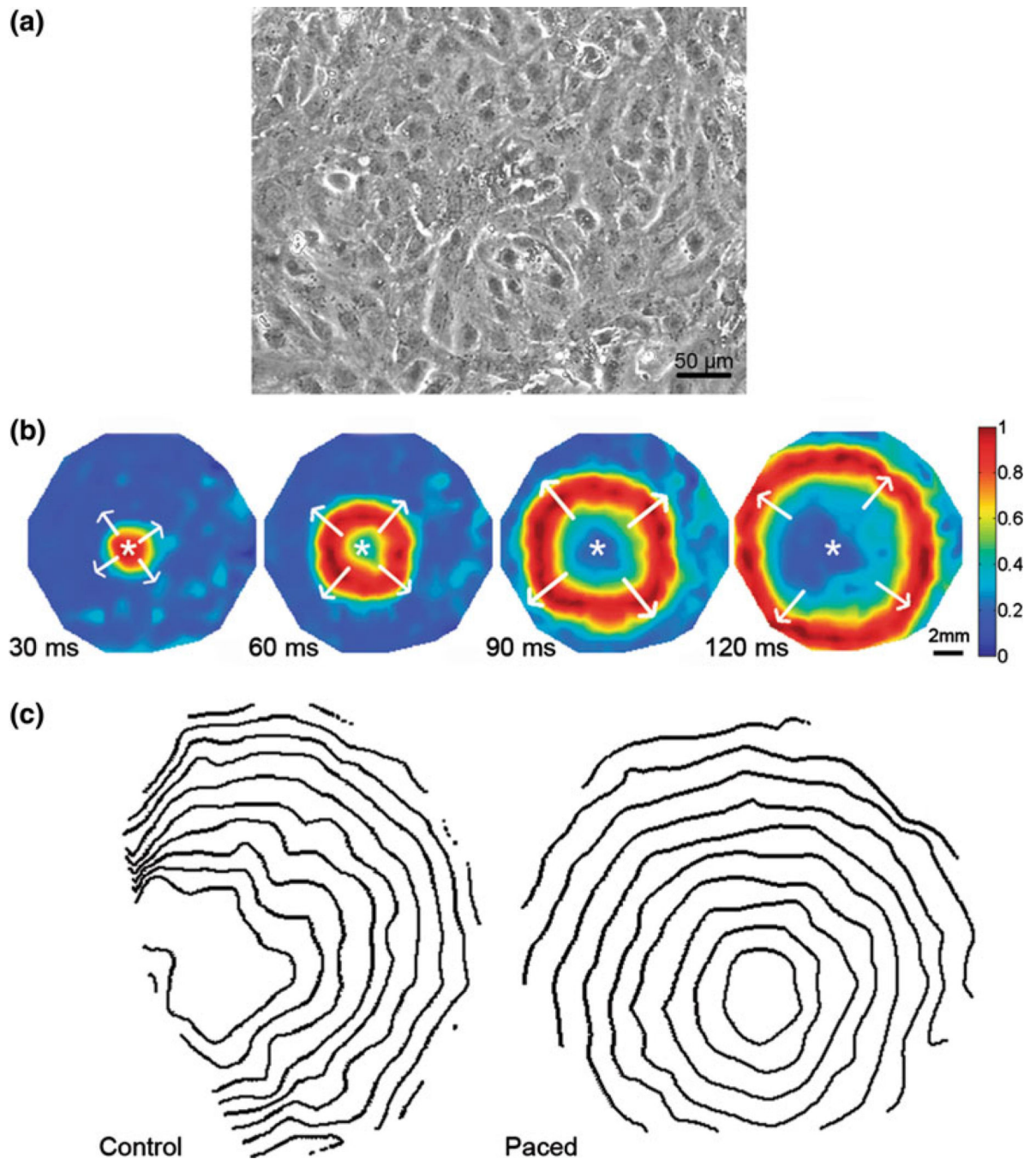
7. Fu JD, Yu HM, Wang R, Liang J, Yang HT. Developmental regulation of intracellular calcium transients during cardiomyocyte differentiation of mouse embryonic stem cells. *Acta Pharmacol. Sin.* 2006; 27:901–910. [PubMed: 16787575]
8. Genovese JA, Spadaccio C, Langer J, Habe J, Jackson J, Patel AN. Electrostimulation induces cardiomyocyte predifferentiation of fibroblasts. *Biochem. Biophys. Res. Commun.* 2008; 370:450–455. [PubMed: 18384743]
9. Genovese JA, Spadaccio C, Chachques E, Schussler O, Carpentier A, Chachques JC, Patel AN. Cardiac pre-differentiation of human mesenchymal stem cells by electrostimulation. *Front Biosci.* 2009; 14:2996–3002.
10. Griffin MA, Sen S, Sweeney HL, Discher DE. Adhesion-contractile balance in myocyte differentiation. *J. Cell Sci.* 2004; 117:5855–5863. [PubMed: 15522893]
11. Gryshchenko O, Fischer IR, Dittrich M, Viatchenko-Karpinski S, Soest J, Bohm-Pinger MM, Igelmund P, Fleischmann BK, Hescheler J. Role of ATP-dependent K(+) channels in the electrical excitability of early embryonic stem cell-derived cardiomyocytes. *J. Cell Sci.* 1999; 112(Pt 17): 2903–2912. [PubMed: 10444385]
12. Guo A, Yang HT. Ca<sup>2+</sup> removal mechanisms in mouse embryonic stem cell-derived cardiomyocytes. *Am. J. Physiol. Cell Physiol.* 2009; 297:C732–C741. [PubMed: 19605739]
13. Heng BC, Haider H, Sim EK, Cao T, Ng SC. Strategies for directing the differentiation of stem cells into the cardiomyogenic lineage in vitro. *Cardiovasc. Res.* 2004; 62:34–42. [PubMed: 15023550]
14. Heron, M., Hoyert, DL., Murphy, SL., Xu, JQ., Kochanek, KD., Tejada-Vera, B. Deaths: Final Data for 2006. Hyattsville, MD: U.S. Department of Health and Human Services, National Center for Health Statistics; 2009.
15. Hescheler J, Fleischmann BK, Lentini S, Maltsev VA, Rohwedel J, Wobus AM, Addicks K. Embryonic stem cells: a model to study structural and functional properties in cardiomyogenesis. *Cardiovasc. Res.* 1997; 36:149–162. [PubMed: 9463627]
16. Inoue N, Ohkusa T, Nao T, Lee JK, Matsumoto T, Hisamatsu Y, Satoh T, Yano M, Yasui K, Kodama I, Matsuzaki M. Rapid electrical stimulation of contraction modulates gap junction protein in neonatal rat cultured cardiomyocytes: involvement of mitogen-activated protein kinases and effects of angiotensin II-receptor antagonist. *J. Am. Coll. Cardiol.* 2004; 44:914–922. [PubMed: 15312880]
17. Itzhaki I, Schiller J, Beyar R, Satin J, Gepstein L. Calcium handling in embryonic stem cell-derived cardiac myocytes: of mice and men. *Ann. NY Acad. Sci.* 2006; 1080:207–215. [PubMed: 17132785]
18. Kapur N, Banach K. Inositol-1, 4, 5-trisphosphate-mediated spontaneous activity in mouse embryonic stem cell-derived cardiomyocytes. *J. Physiol.* 2007; 581:1113–1127. [PubMed: 17379641]
19. Klug MG, Soonpaa MH, Koh GY, Field LJ. Genetically selected cardiomyocytes from differentiating embryonic stem cells form stable intracardiac grafts. *J. Clin. Invest.* 1996; 98:216–224. [PubMed: 8690796]
20. Kolossov E, Lu Z, Drobinskaya I, Gassanov N, Duan Y, Sauer H, Manzke O, Bloch W, Bohlen H, Hescheler J, Fleischmann BK. Identification and characterization of embryonic stem cell-derived pacemaker and atrial cardiomyocytes. *FASEB J.* 2005; 19:577–579. [PubMed: 15659535]
21. Kolossov E, Bostani T, Roell W, Breitbach M, Pillekamp F, Nygren JM, Sasse P, Rubenchik O, Fries JW, Wenzel D, Geisen C, Xia Y, Lu Z, Duan Y, Kettenhofen R, Jovinge S, Bloch W, Bohlen H, Welz A, Hescheler J, Jacobsen SE, Fleischmann BK. Engraftment of engineered ES cell-derived cardiomyocytes but not BM cells restores contractile function to the infarcted myocardium. *J. Exp. Med.* 2006; 203:2315–2327. [PubMed: 16954371]
22. Kraus RL, Li Y, Jovanovska A, Renger JJ. Trazodone inhibits T-type calcium channels. *Neuropharmacology.* 2007; 53:308–317. [PubMed: 17610910]
23. Lammers WJ, Schalij MJ, Kirchhof CJ, Allesie MA. Quantification of spatial inhomogeneity in conduction and initiation of reentrant atrial arrhythmias. *Am. J. Physiol.* 1990; 259:H1254–H1263. [PubMed: 1699438]



24. Martens JC, Radmacher M. Softening of the actin cytoskeleton by inhibition of myosin II. *Pflugers Arch.* 2008; 456:95–100. [PubMed: 18231808]
25. Nichol JW, Engelmayr GC Jr, Cheng M, Freed LE. Co-culture induces alignment in engineered cardiac constructs via MMP-2 expression. *Biochem. Biophys. Res. Commun.* 2008; 373:360–365. [PubMed: 18559256]
26. Pedrotty DM, Koh J, Davis BH, Taylor DA, Wolf P, Niklason LE. Engineering skeletal myoblasts: roles of three-dimensional culture and electrical stimulation. *Am. J. Physiol. Heart Circ. Physiol.* 2005; 288:H1620–H1626. [PubMed: 15550526]
27. Radisic M, Park H, Shing H, Consi T, Schoen FJ, Langer R, Freed LE, Vunjak-Novakovic G. Functional assembly of engineered myocardium by electrical stimulation of cardiac myocytes cultured on scaffolds. *Proc. Natl Acad. Sci. USA.* 2004; 101:18129–18134. [PubMed: 15604141]
28. Sathaye, AS. Effects of Long Term Electrical Stimulation on the Electrophysiological Development of Neonatal Rat Ventricular Myocytes [Master's thesis]. Johns Hopkins University: 2003.
29. Sauer H, Rahimi G, Hescheler J, Wartenberg M. Effects of electrical fields on cardiomyocyte differentiation of embryonic stem cells. *J. Cell Biochem.* 1999; 75:710–723. [PubMed: 10572253]
30. Tung L, Zhang Y. Optical imaging of arrhythmias in tissue culture. *J. Electrocardiol.* 2006; 39:S2–S6. [PubMed: 17015066]
31. Weiss JN, Qu Z, Chen PS, Lin SF, Kara-gueuzian HS, Hayashi H, Garfinkel A, Karma A. The dynamics of cardiac fibrillation. *Circulation.* 2005; 112:1232–1240. [PubMed: 16116073]
32. Wobus AM, Guan K, Yang HT, Boheler KR. Embryonic stem cells as a model to study cardiac, skeletal muscle, and vascular smooth muscle cell differentiation. *Methods Mol. Biol.* 2002; 185:127–156. [PubMed: 11768985]
33. Xia Y, McMillin JB, Lewis A, Moore M, Zhu WG, Williams RS, Kellems RE. Electrical stimulation of neonatal cardiac myocytes activates the NFAT3 and GATA4 pathways and up-regulates the adenylosuccinate synthetase 1 gene. *J. Biol. Chem.* 2000; 275:1855–1863. [PubMed: 10636885]
34. Yanagi K, Takano M, Narazaki G, Uosaki H, Hoshino T, Ishii T, Misaki T, Yamashita JK. Hyperpolarization-activated cyclic nucleotide-gated channels and T-type calcium channels confer automaticity of embryonic stem cell-derived cardiomyocytes. *Stem Cells.* 2007; 25:2712–2719. [PubMed: 17656646]
35. Zhang YM, Shang L, Hartzell C, Narlow M, Cribbs L, Dudley SC Jr. Characterization and regulation of T-type Ca<sup>2+</sup> channels in embryonic stem cell-derived cardiomyocytes. *Am. J. Physiol. Heart Circ. Physiol.* 2003; 285:H2770–H2779. [PubMed: 12919937]
36. Zimmermann WH. Tissue engineering: polymers flex their muscles. *Nat. Mater.* 2008; 7:932–933. [PubMed: 19029926]



**FIGURE 1.**  
Experimental timeline.

**FIGURE 2.**

Electrical conduction in confluent monolayers of mESC-CMs. (a) Phase contrast image of monolayer taken at 103. (b) Voltage maps show wave propagation from point of stimulation marked with a white asterisk. The stimulus pulse is given at time 0 ms. Each panel shows wavefront at different times after the stimulus pulse was applied. Spectrum of colors represents normalized voltage from blue (lowest) to red (highest). Scale bar (2 mm) represents physical length on the coverslip. (c) Isochrone maps show wavefronts at 13-ms time intervals. The average CVs in these examples were 6.46 cm/s for the control (left panel)

and 6.56 cm/s for paced mESC-CMs (right panel). Isochrones of paced monolayers (HI = 1.18) are smoother than those of non-paced monolayers (HI = 2.68).

Author Manuscript

Author Manuscript

Author Manuscript

Author Manuscript

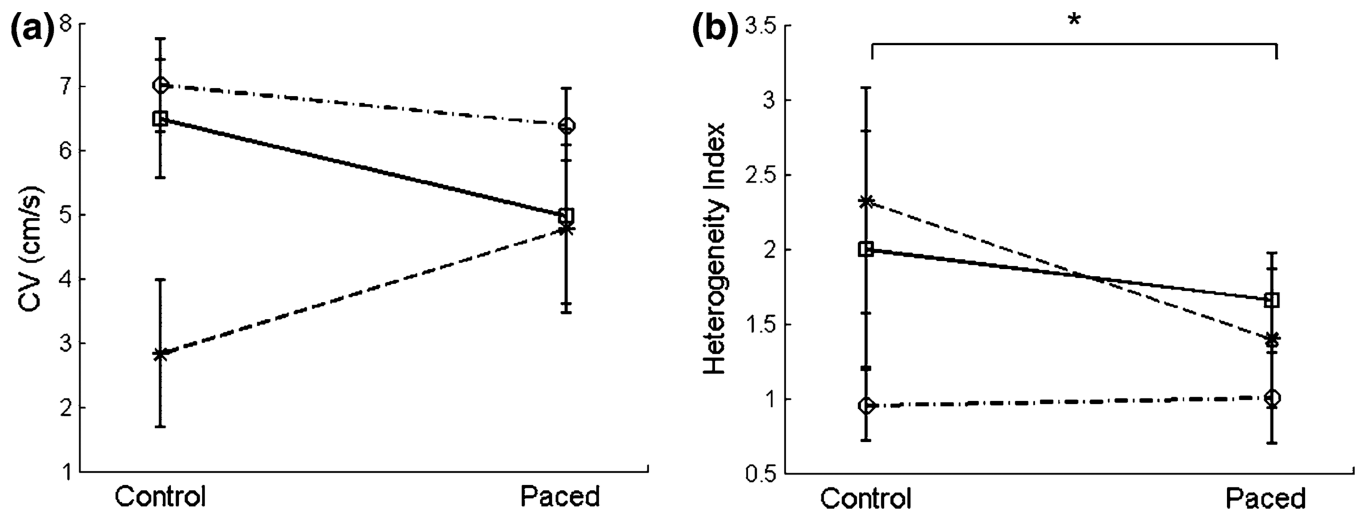


**FIGURE 3.**

Electrical conduction in paced mESC-CM monolayers. (a) Average batch conduction velocities (CVs) of control and paced mESC-CMs on day 19 at a 4-Hz stimulation rate. Different lines signify different differentiation batches. No significant difference was found in CVs between control and paced mESC-CMs. (b) Heterogeneity index (HI) of the individual control and paced monolayers of (a). In (a) and (b), variation in CV at two levels of tissue organization is shown: (a) shows the reduction of variation in CV among differentiation batches in paced mESC-CMs compared to control, while (b) shows the reduction of variation within monolayers (heterogeneity index) in paced mESC-CMs indicating more uniform intercellular electrical coupling ( $p$  value = 0.0001). Data from eight control and seven paced monolayers from three differentiation batches. \* $p < 0.05$ .



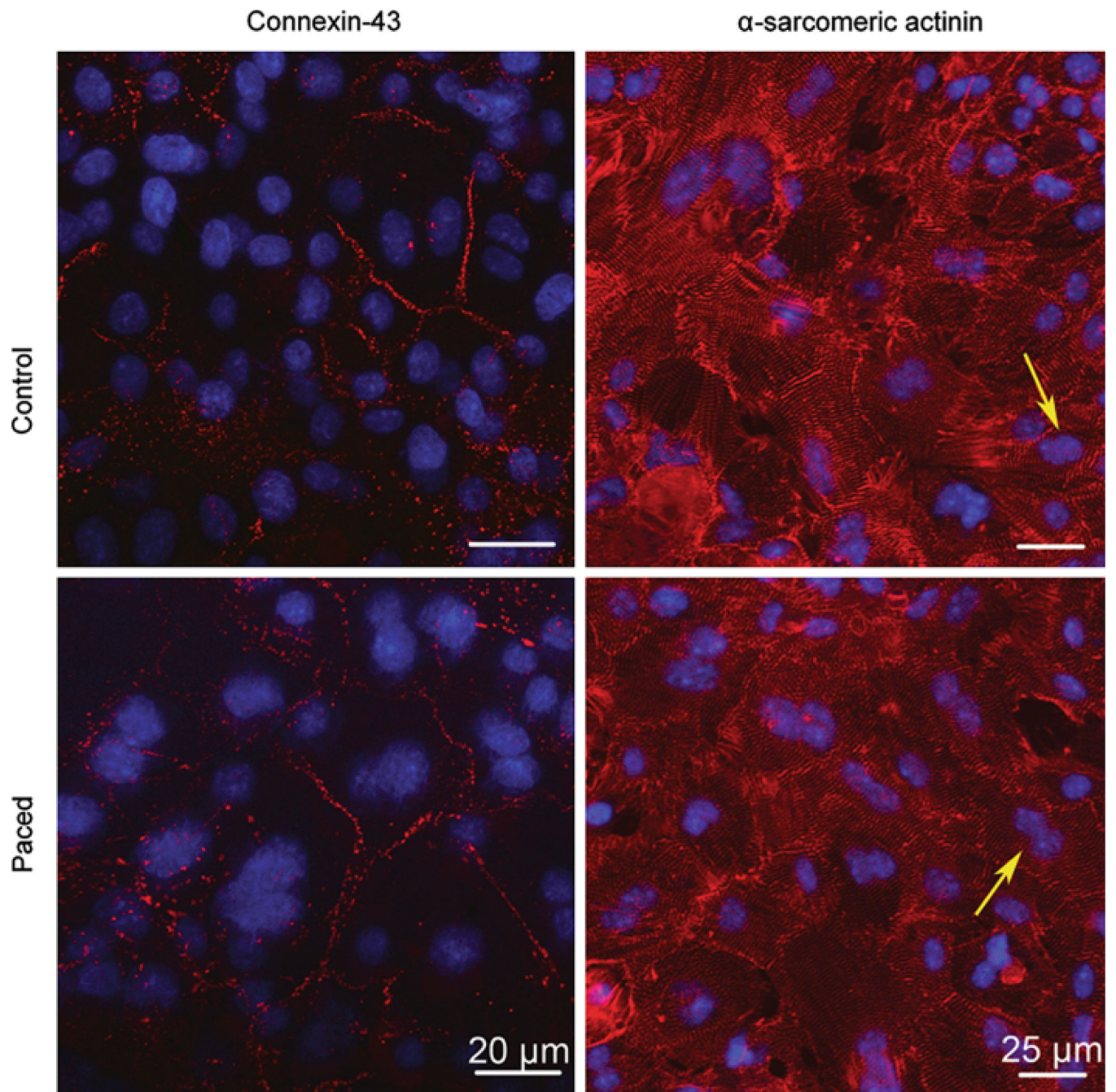


**FIGURE 4.** Immunohistochemistry for control and paced mESC-CMs on day 19 following optical mapping. Upper row is control and lower row is paced. Left column are immunofluorescent images of connexin-43 staining taken at 603 with a confocal microscope and right column are images of  $\alpha$ -sarcomeric actinin taken at 40 $\times$  with a confocal microscope and further zoomed in digitally at 2 $\times$ . There was no apparent difference in either the distribution of gap junctions or the morphology of non-paced and paced mESC-CMs. Notice the presence of binucleated cells indicated by yellow arrows.



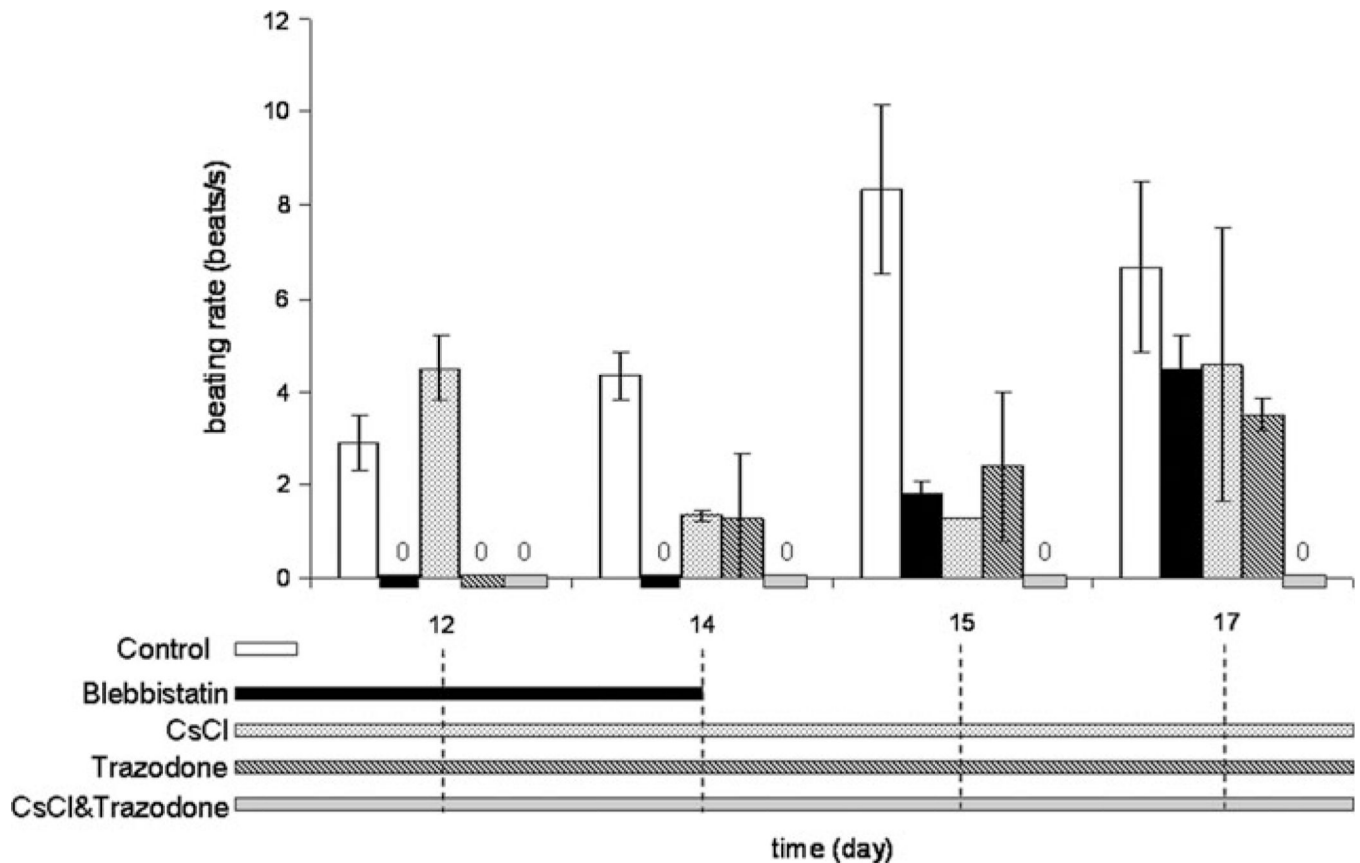


**FIGURE 5.**

Spontaneous beating rate of mESC-CMs observed from day 12 to 17. The bars represent different drug treatments and duration of the treatment, corresponding to the timeline on the horizontal axis of the bar graphs. The spontaneous beating rate of control mESC-CMs increases and then decreases over time. Beating was completely suppressed by blebbistatin (days 11–14) and resumed with blebbistatin washout, although at a slower rate than in control. The beating rate was only partially suppressed by CsCl, and initially was completely suppressed by trazodone, although beating returned on days 14–17. The combination of trazodone and CsCl suppressed beating throughout the whole course of treatment. Data are from a total of seven control monolayers and four monolayers per drug-treated group from two differentiation batches.

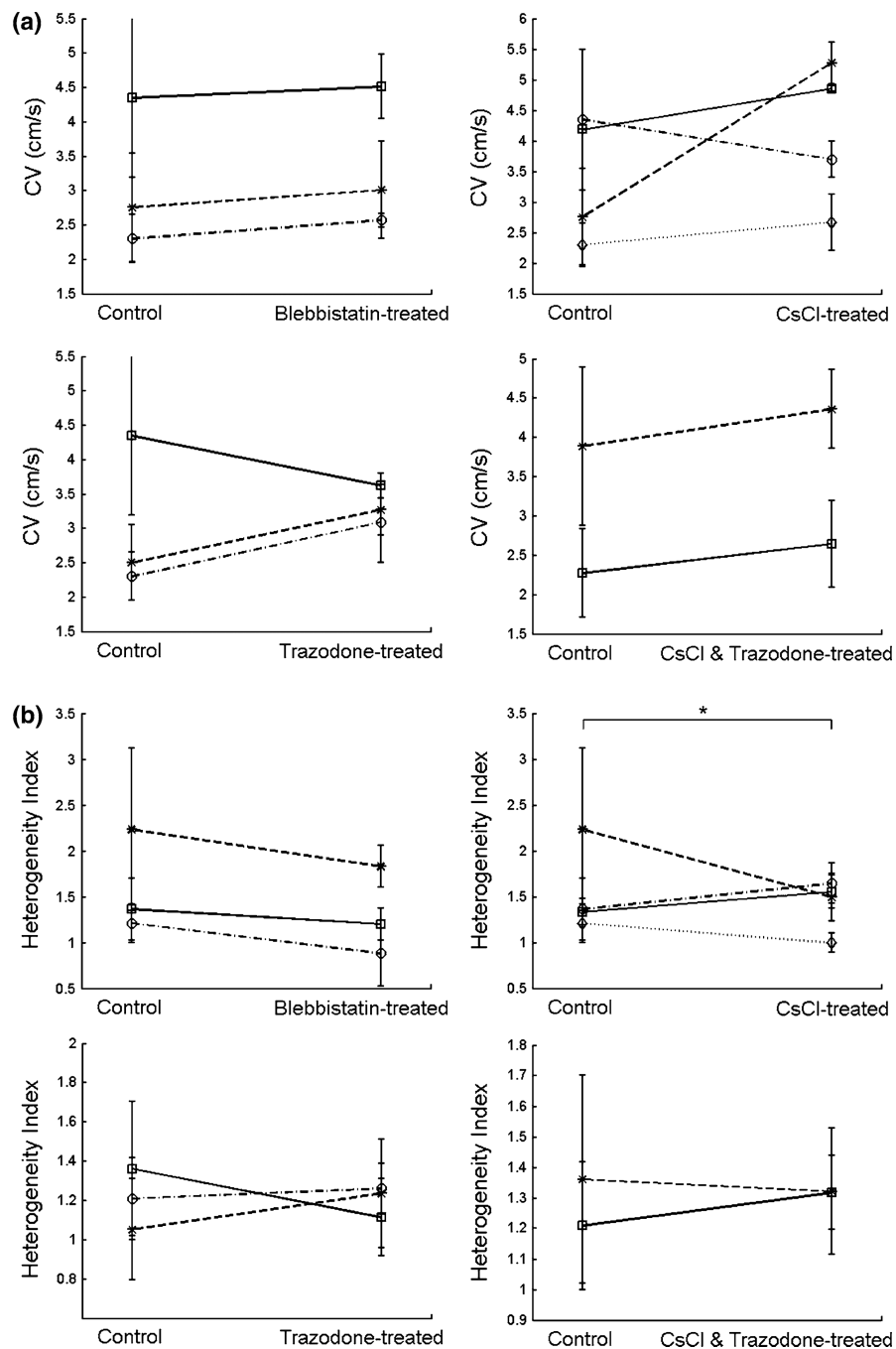


**FIGURE 6. Electrical conduction in mESC-CM monolayers with suppressed spontaneous contraction**

(a) Average conduction velocities (CVs) of control and mESC-CMs with suppressed contraction on day 18 at a 5-Hz stimulation rate for blebbistatin-, CsCl-, and trazodone-treated mESC-CMs and at a 6-Hz stimulation rate for the combination of CsCl and trazodone treatment. Different lines signify different differentiation batches. No significant differences of CVs were found between control and mESC-CMs with suppressed contraction. (b) Heterogeneity index (HI) of the individual control and mESC-CM monolayers of (a). In (a) and (b), variation in CV at two levels of tissue organization is

shown. (a) CV variation among differentiation batches in drug-treated mESC-CMs compared to control. Only the variance of conduction velocities for trazodone-treated mESC-CM monolayers was found to be significantly different from the variance of control ( $p < 0.0001$ ). (b) CV variation within monolayers (heterogeneity index) in control and drug-treated mESC-CMs. Only CsCl-treated mESC-CMs showed significantly lower HI compared with control ( $p$  value = 0.038). Data are from seven control, six drug-treated, and three differentiation batches for blebbistatin; 7, 10, and 4 for CsCl; 6, 10, and 3 for trazodone; and 5, 4, and 2 for CsCl combined with trazodone.  $*p < 0.05$ .

Author Manuscript

Author Manuscript

Author Manuscript

Author Manuscript

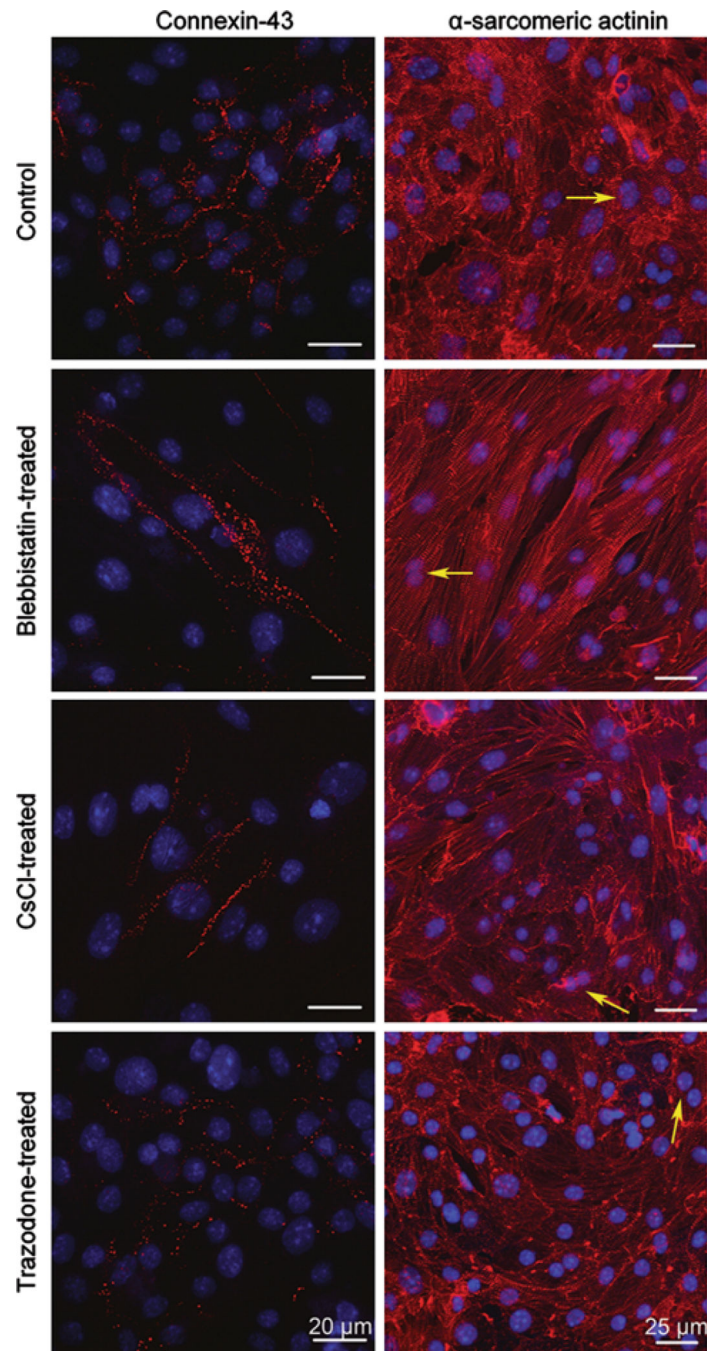


**FIGURE 7.** Immunohistochemistry for control and drug-treated mESC-CMs on day 18 following optical mapping. Left column are immunofluorescent images of connexin-43 staining taken at 60× with a confocal microscope and right column are images of  $\alpha$ -sarcomeric actinin taken at 40× with a con-focal microscope and further zoomed in digitally at 2×. Blebbistatin-treated mESC-CMs were washed free of blebb-istatin on day 15 and regained confluency with a rod-shaped morphology (second row). The morphologies of CsCl- and trazodone-treated

mESC-CMs were similar to those of control (third and fourth rows). Notice the presence of binucleated cells indicated by yellow arrows.

Author Manuscript

Author Manuscript

Author Manuscript

Author Manuscript

**TABLE 1**

Primer sequences for RT-PCR.

| Gene product | Forward                  | Reverse                   |
|--------------|--------------------------|---------------------------|
| GAPDH        | TTCCAGTATGACTCCACTCACGG  | TGAAGACACCAGTAGACTCCACGAC |
| NCX          | AGATCAAGCATCTGCGTGTG     | TGGAAGCTGGTCTGTCTCCT      |
| Cx43         | GTGGCCTGCTGAGAACCTAC     | GAGCGAGAGACACCAAGGAC      |
| AlphaMHC     | TGGCCAAGTCAGTGTACGAG     | CGAACATGTGGTGGTTGAAG      |
| BetaMHC      | TGCAAAGGCTCCAGGTCTGAGGGC | GCCAACACCAACCTGTCCAAGTTC  |
| Cav3.1       | ACCCTCCCAAAGAAAGAT       | GCTTACATGGGACTTTTCAG      |
| Cav3.2       | GCTGTTTGGGAGGCTAGAAT     | CGAAGGTGACGAAGTAGACG      |
| HCN1         | TGCTGTGCATTGGGTATGGA     | TTTCGGCAGTTAAAGTTGATG     |

Author Manuscript

Author Manuscript

Author Manuscript

Author Manuscript